PB89-206668

Air Pollution Climatology Around an Isolated Point Source Using Convective Scaling Parameters

(U.S.) Environmental Protection Agency, Research Triangle Park, NC

1988

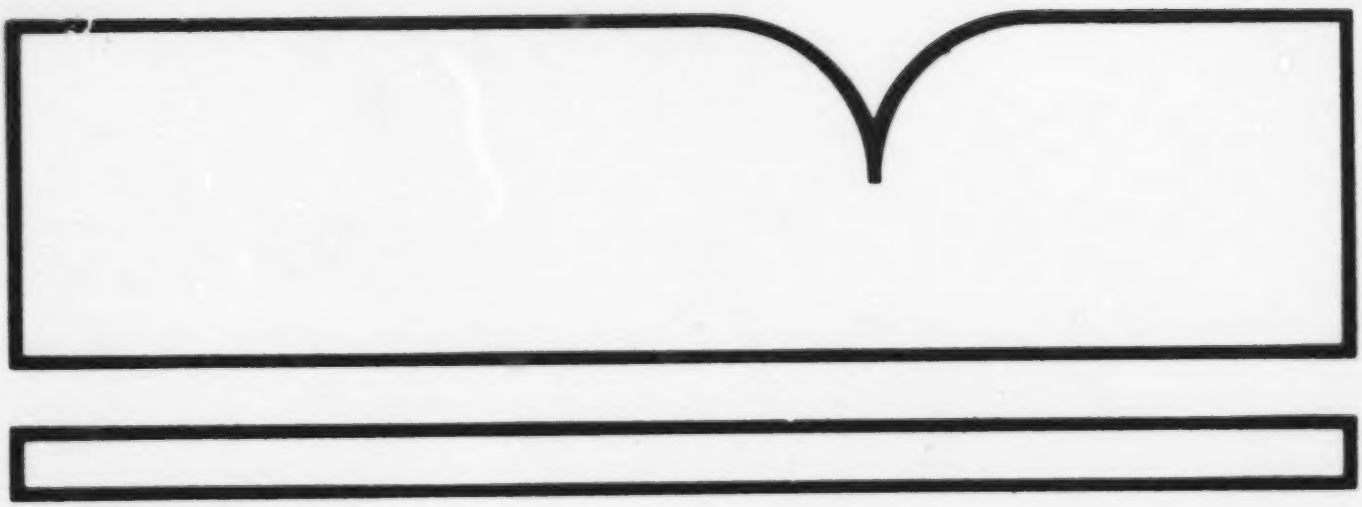

U.S. Department of Commerce
National Technical Information Service
NTIS

TECHNICAL REPORT DATA
(Please read Instructions on the reverse before completing)

1. REPORT NO.	2.	3. RE PB89-206668
EPA/600/J-88/333		

4. TITLE AND SUBTITLE
AN AIR POLLUTION CLIMATOLOGY OF AN ISOLATED POINT SOURCE USING CONVECTIVE SCALING PARAMETERS

5. REPORT DATE

6. PERFORMING ORGANIZATION CODE

7. AUTHOR(S)
Thomas E. Pierce

8. PERFORMING ORGANIZATION REPORT NO.

9. PERFORMING ORGANIZATION NAME AND ADDRESS
Atmospheric Sciences Research Laboratory
Office of Research and Development
U.S. Environmnetal Protection Agency
Research Triangle Park, NC 27711

10. PROGRAM ELEMENT NO.
A101/B65/04-6239 (FY-87)

11. CONTRACT/GRANT NO.

12. SPONSORING AGENCY NAME AND ADDRESS
Atmospheric Sciences Research Laboratory--RTP,NC
Office of Research and Development
U. S. Environmental Protection Agency
Research Triangle Park, NC 27711

13. TYPE OF REPORT AND PERIOD COVERED
In-house (12/86-8/87)

14. SPONSORING AGENCY CODE
EPA/600/09

15. SUPPLEMENTARY NOTES
Atmospheric Environment, Vol. 22, No. 11, pp. 2463-2475, 1988

16. ABSTRACT

An air pollution climatology, which incorporated convective scaling parameters, is used to investigate the conditions associated with hourly sulfur dioxide concentrations from a coal-fired power plant. One year of data from the Paradise power plant in central Kentucky (U.S.A.) was analyzed. Variables which were examined included emission rate, plume rise, wind speed, wind direction, stability class, convective scaling velocity, and similarity categories. The results show the meteorological conditions leading to high surface concentrations are the daytime hours having neutral/unstable atmospheric stability, light winds, and effective plume height to mixing height ratios typically greater than 0.85. In more than half of the 30 hours of highest observed concentrations, the atmospheric conditions satisfy the criteria for mixed-layer scaling.

17. KEY WORDS AND DOCUMENT ANALYSIS

a. DESCRIPTORS	b. IDENTIFIERS/OPEN ENDED TERMS	c. COSATI Field/Group

REPRODUCED BY
U.S. DEPARTMENT OF COMMERCE
NATIONAL TECHNICAL INFORMATION SERVICE
SPRINGFIELD, VA. 22161

18. DISTRIBUTION STATEMENT	19. SECURITY CLASS (This Report)	21. NO. OF PAGES
RELEASE TO PUBLIC	UNCLASSIFIED	15
	20. SECURITY CLASS (This page) UNCLASSIFIED	22. PRICE MF A01/3.95 6.95

EPA Form 2220-1 (Rev. 4-77) PREVIOUS EDITION IS OBSOLETE

EPA/600/J-88/333

Atmospheric Environment Vol. 22, No. 11, pp. 2463–247?, 1988.
Printed in Great Britain.

0004-6981/88 $3.00 + 0.00
Pergamon Press plc

AN AIR POLLUTION CLIMATOLOGY AROUND AN ISOLATED POINT SOURCE USING CONVECTIVE SCALING PARAMETERS

THOMAS E. PIERCE*

Atmospheric Sciences Research Laboratory, U.S. Environmental Protection Agency, Research Triangle Park, NC 27711, U.S.A.

(*First received* 17 *August* 1987 *and in final form* 28 *March* 1988)

Abstract—An air pollution climatology, which incorporated convective scaling parameters, is used to investigate the conditions associated with hourly SO_2 concentrations from a coal-fired power plant. One year of data from the Paradise power plant in central Kentucky (U.S.A.) were analyzed. Variables which were examined included emission rate, plume rise, wind speed, wind direction, stability class, convective scaling velocity and similarity categories. The results show the meteorological conditions leading to high surface concentrations are the daytime hours having neutral/unstable atmospheric stability, light winds and effective plume height to mixing height ratios typically > 0.85. In more than half of the 30 h of highest observed concentrations, the atmospheric conditions satisfy the criteria for mixed-layer scaling.

Key word index: Air pollution climatology, similarity scaling, convective boundary layer, tall stack modeling, coal-fired power plant.

1. INTRODUCTION

Atmospheric pollution modeling has become an integral part of environmental protection. Users, however, must select from a vast assortment of atmospheric pollution models. Furthermore, the model selected for application should be able to simulate diffusion for a range of meteorological conditions, especially those associated with elevated pollution levels. Identifying the important meteorological regimes, and therefore the appropriate atmospheric pollution model, can be determined from an air pollution climatology.

Holzworth (1987) noted that an air pollution climatology "primarily deals with descriptors of meteorologic factors that are important in the occurrence of large or undesirable concentrations of atmospheric pollutants." Traditionally, air pollution climatologies have been limited to basic variables such as wind speed, wind direction, mixing height and stability class. In this paper, an air pollution climatology will be extended to include mixed-layer scaling.

Over the past 15 years, mixed-layer scaling has gradually been incorporated into atmospheric pollution models. Deardorff (1970) introduced mixed-layer scaling, noting that diffusion in the convective boundary layer could be scaled by the mixed-layer height (h) and the convective scaling velocity (w_*). Significant progress by including mixed-layer scaling into atmospheric pollution models was made by Venkatram (1980) and Weil and Brower (1984). Plume buoyancy effects were later accounted for by Briggs (1985). Briggs's parameterizations have since been successfully used by Weil *et al.* (1986), Pierce (1986) and Hanna *et al.* (1987). Gryning *et al.* (1987) argue for future routinely-applied models to incorporate mixed-layer scaling.

Climatologies using mixed-layer scaling have been reported by Lee (1986) and Ning and Yap (1986). However, these types of climatological analyses did not include a comparison of climatic data with observed pollution levels. This paper reports on an air pollution climatology using convective parameters to investigate elevated SO_2 concentrations observed around an isolated coal-fired power plant. By examining the observed concentrations in the framework of an air pollution climatology, some insight is gained on identifying the meteorological factors of importance for tall stack models.

2. DATA

Data for this analysis were taken from the Paradise coal-fired power plant in central Kentucky (Fig. 1). Paradise is a 2600 MW base-line facility operated by the Tennessee Valley Authority (TVA). TVA supported an extensive monitoring program in which they collected hourly source, meteorological and SO_2 concentration data during 1976.

Exhaust gases from Paradise were vented out of three stacks: two of which were 183 m in height and the third was 244 m. Operating characteristics for

*On assignment from the National Oceanic and Atmospheric Administration, U.S. Department of Commerce.

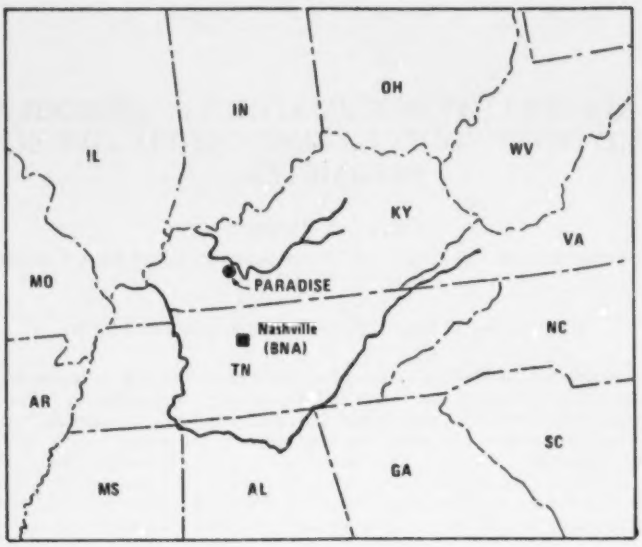

Fig 1. Regional overview of the Paradise power plant.

Table 1. Stack characteristics of the Paradise TVA power plant

Parameter	Stack number 1	2	3
Height (m)	182.9	182.9	243.8
Diameter (m)	7.9	7.9	8.2
Gas temperature (K)			
100% capacity	416.5	416.5	423.7
75% capacity	412.6	412.6	413.7
50% capacity	410.4	410.4	405.9
Exit velocity ($m s^{-1}$)			
100% capacity	17.1	17.1	26.1
75% capacity	13.2	13.2	18.8
50% capacity	9.2	9.2	14.2
Generating capacity (MW)	704	704	1150

each stack are summarized in Table 1. For the analysis, daily average SO_2 emission rates and stack operating characteristics were determined from daily coal consumption values from each stack. The S content of the coal was analyzed weekly.

Meteorological measurements were taken from a 110 m tower located 1.5 km west of the power plant as shown in Fig. 2. Available on-site meteorological data included hourly averages of wind speed, wind direction and ambient air temperature. Additional meteorological data for 1976 were obtained from the National Weather Service station at Nashville, Tennessee (BNA), located about 100 km south of Paradise. Surface observations were available on an hourly basis and upper-air data were available twice-daily at 00 GMT and 12 GMT.

Hourly SO_2 concentrations were measured at 12 monitors situated around the plant as shown in Fig. 2. The azimuth, distance from the plant, relative height above stack base and percentage of valid data collected during 1976 are listed in Table 2.

3. METHODS FOR ANALYSIS

For this analysis, a variety of variables were compared to measured SO_2 concentrations. Most of these were meteorological variables used in atmospheric pollution models. Some variables such as wind speed and wind direction were obtained from direct measurements. Other variables were determined indirectly: including synoptic class, mixing height, stability class, plume rise, similarity parameters and convective scaling velocity. Briefly, the methods used for estimating these variables are discussed below.

3.1. *Synoptic class*

Yu and Pielke (1986) reported on a synoptic typing scheme used for classifying air quality in a mesoscale region of the western U.S. Their scheme was modified for this study to include stationary fronts which are common in the estern U.S. The modified scheme is as follows:

Category 1—warm sector of an extratropical cyclone.
Category 2—ahead of a warm front, cyclonic flow.
Category 3—behind a cold front, cyclonic flow.
Category 4—under a polar high, anticyclonic flow.
Category 5—vicinity of a subtropical ridge.
Category 6—vicinity of a stationary front.

Table 2. Site characteristics and data acquisition of the Paradise SO_2 monitors during 1976

Receptor number	Azimuth (degrees)	Distance (km)	Height above plant grade (m)	Percentage of missing data ($n = 8784$ h)
1	31	2.9	−1	62.1
2	47	16.9	24	61.4
3	31	4.7	21	3.7
4	31	6.8	36	61.6
5	32	8.4	15	61.6
6	284	12.7	12	1.8
7	126	8.5	−7	1.4
8	301	3.4	16	2.8
9	150	7.0	15	1.8
10	238	7.7	22	0.3
11	342	6.1	2	0.6
12	179	7.9	10	0.6

The motivation for using such a scheme is to determine if elevated pollution levels could be associated with distinct synoptic conditions.

3.2. *Mixed-layer height*

Hourly mixed-layer heights for 1976 were determined from the twice-daily BNA upper-air soundings using the E.P.A. (1977) method. This procedure was selected because it is routinely used in atmospheric pollution modeling.

3.3. *Stability class*

Using the surface observations from BNA, Pasquill stability classes were determined using the methods described by Turner (1964).

3.4. *Plume rise*

Plume rise for each stack was estimated using the methods of Briggs given in the CRSTER dispersion model (E.P.A., 1977).

In addition, revised estimates of plume rise for the highest 30 h of concentrations were made using the methods of Briggs (1984). His more recent equations incorporate similarity-scaling parameters (Equations 8.97 and 8.101), variations of atmospheric stability with height (Equation 8.84) and partial plume penetration (Equation 8.83). Plume rise enhancement due to merging plumes was not considered because of the relatively large separation distance (180 m) between the stacks.

3.5. *Similarity parameters*

Similarity parameters computed included the friction velocity, u_*, and the Monin–Obukhov length, L. The methods for computing the similarity parameters were based on the U.S. Environmental Protection Agency's Meteorological Processor for Dispersion Analysis (MPDA) developed by Paumier *et al.* (1986).

3.6. *Mixed-layer scaling parameters*

From the similarity parameters, the mixed-layer scaling parameters w_* and F_* were determined. The method for determining the mixing height is discussed above.

The convective scaling velocity w_* can be defined as follows:

$$w_* = \left[\frac{g}{\rho c_p T} H_0 h\right]^{1/3} \tag{1}$$

where g is gravitational acceleration, ρ is the density of air, c_p is the specific heat of air at a constant pressure, T is the ambient air temperature and H_0 is the surface sensible heat flux. Hourly values for H_0 were determined using the methods of Holtslag and van Ulden (1983). The data needed for their scheme were obtained from the on-site data and the BNA surface observations.

The non-dimensional plume buoyancy, F_*, discussed by Venkatram (1980), was also computed. It is defined as follows:

$$F_* = F_b/(\bar{u} w_*^2 h) \tag{2}$$

where F_b is buoyancy flux parameter, and $\bar{u}$ is the average wind speed in the convective boundary layer.

4. ANALYSIS

The first step in the analysis was to compile a data set consisting of one year of hourly monitored SO_2 concentrations. A cumulative frequency distribution of the maximum hourly SO_2 concentrations is shown in Fig. 3. The hourly concentrations ranged from a high of 1120 ppb to 130 ppb at the 95 percentile. Slightly less than 50 per cent of the hours were associated with measurable SO_2 concentrations.

The next step in the analysis was to divide the 8784 h of data into two groups: the top 30 h and the lower 8754 h. Relative concentrations (concentration divided by emission rate) were considered, but the top 30 h were found to be very similar to the actual observed concentrations. The conditions associated with the top 30 h are summarized in Table 3.

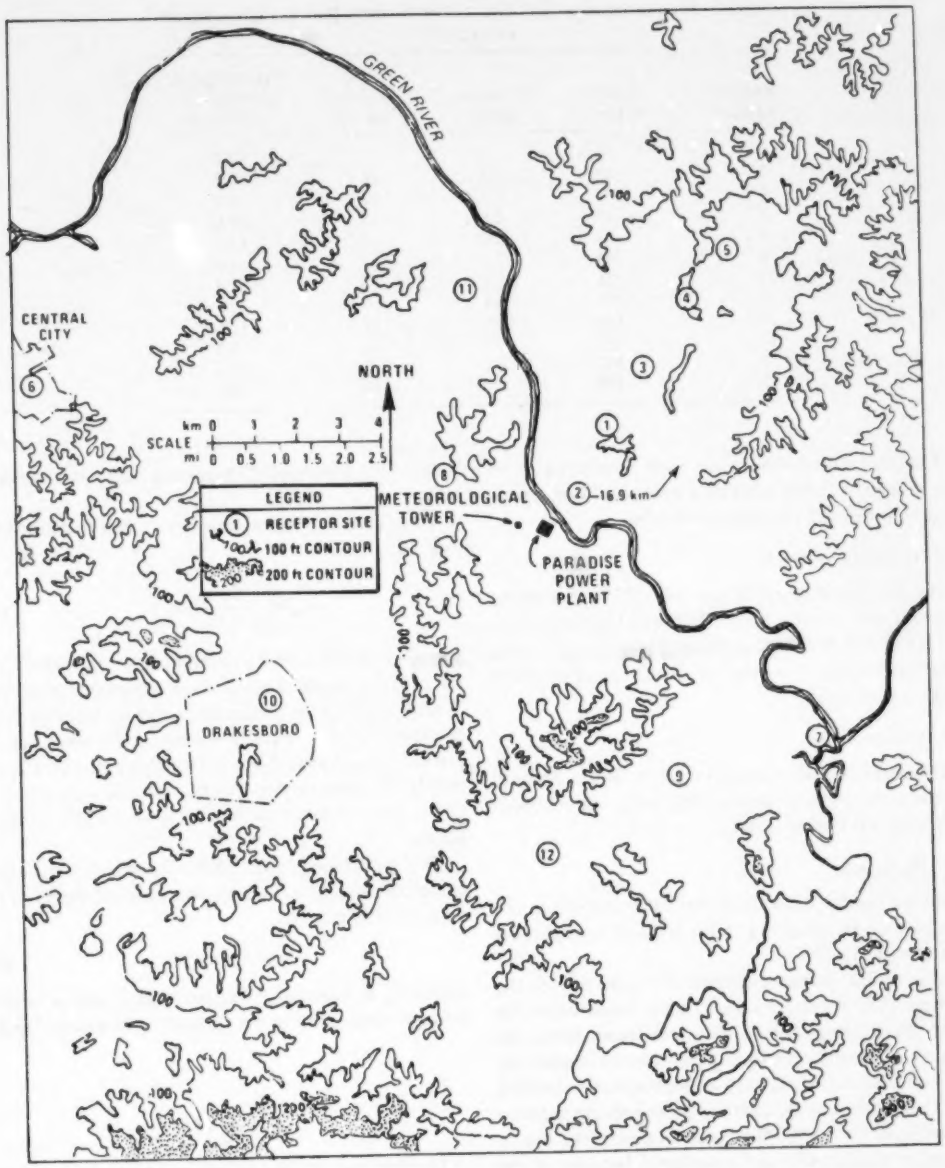

Fig. 2. Paradise power plant site and local surroundings.

With the two data sets, the analysis proceeded as follows. For each data set, hourly values of each variable were sorted into bins, which ranged in size from 3 to 6. As mentioned in section 3, variables of interest included various meteorological and source-related factors. A frequency distribution was determined from the number of hours accumulated in each bin. Each frequency distribution was examined, and then the frequency distributions for the two data sets were compared. The comparison of the top 30 h data set and the lower 8754 h data set was made using a chi-square statistic on the normalized frequency distributions. The frequency distributions and their comparisons for each variable are given in Table 4.

4.1. *Emission rate*

Higher concentrations are usually expected with increased emission rates. However, because reduced plant loads are usually associated with lower emission rates, this expectation was not realized from the analysis. The emission rates for the 8754 h data set approximately fit a normal distribution with a median

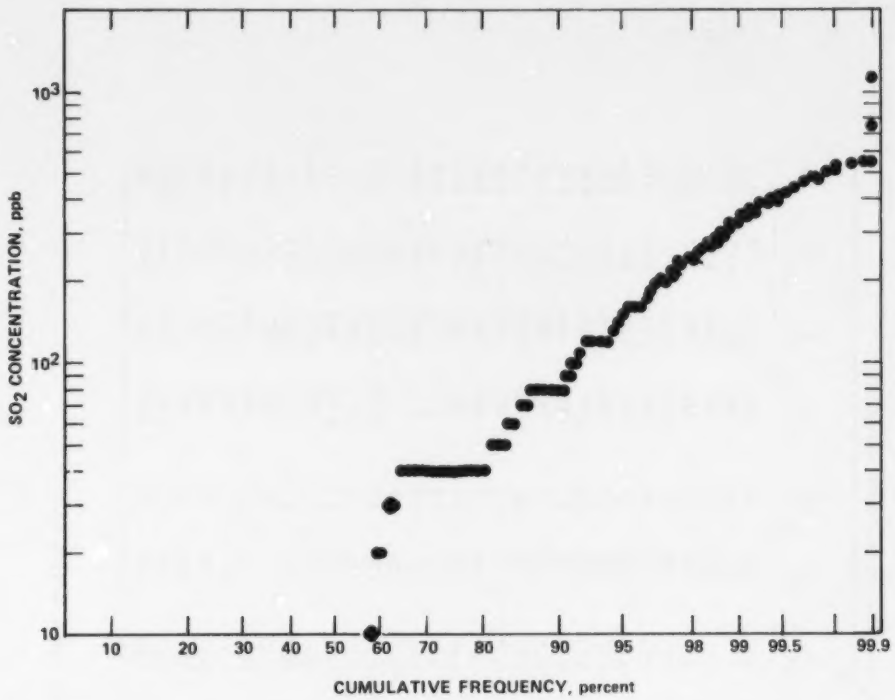

Fig. 3. Cumulative frequency distribution of the maximum hourly concentrations. Note that only every third data point (out of 8784 h of data) is plotted.

in the range of 10 to 15 kg s^{-1}. For the top 30 h data set, the median emission rate was in the range 15 to 20 kg s^{-1}. However, high concentrations were also observed during low emission rates. Furthermore, the frequency distributions of the two data sets were not significantly different as determined with a chi-square statistic. This supports the modeling results of Irwin and Cope (1979) who showed that a reduced plant load (smaller buoyancy flux and emission rate) can lead to higher ground-level concentrations, as the lower buoyancy flux results in lower plume rise. With the lower plume rise, plume penetration into elevated inversions occurs less frequently, also perhaps accounting for some of the high concentrations observed during reduced emissions.

4.2. *Distance*

Table 4 also indicates the distribution of high concentrations as a function of distance. Unfortunately, only 12 monitoring locations were available at Paradise, and four of these locations collected only a limited amount of data. The number of hours reported for the lower 8754 h data set in Table 4 represents the total amount of valid data available from the monitoring network (minus the 30 h of high concentrations). The data were sorted into four distance categories: close (< 4 km), moderately close (4–7 km), moderately far (7–10 km) and far (> 10 km). Most of the data were collected at the moderate distances. The top 30 h appear to be evenly distributed as a function of distance. A chi-square test did not detect any significant differences between the lower 8754 h distribution and the top 30 h distribution. These results tend to substantiate observations reported by Bowne and Londergan (1983) that high pollution levels from a tall stack can occur over a wide range of distances.

4.3. *Synoptic class*

From the analysis, category 4 predominated both the lower 8754 h and top 30 h data sets. Category 4 is typified by an elevated subsidence inversion and light winds. More than 50 per cent of the lower 8754 h were associated with category 4 conditions. More frequently, however, it occurred with the top 30 h 85 per cent of the time. In Table 4, frequencies of 0.5 indicate that for an hour that the synoptic conditions could not be resolved between two categories; thus, a frequency of 0.5 was assigned to both categories. It should be noted that high concentrations were not reported during favorable diffusive conditions, categories 1 and 2.

4.4. *Wind speed*

Wind speeds were divided into five categories as noted in Table 4. The median value for the 8754 h data base was for moderate winds (6–8 m s^{-1}), while the median value for the top 30 h data base was for light

Table 3. Conditions associated with the highest 30 h of SO_2 concentrations at Paradise during 1976

Date	Hour	Conc. (ppb)	Recep. no.	110 m $\bar{u}$ ($m\,s^{-1}$)	PG class	h (m)	Synoptic class	H_o ($W\,m^2$)	u_* (ms^{-1})	L (m)	w_* ($m\,s^{-1}$)	F_b ($m^4\,s^{-3}$)	$\bar{h}_c$ (m)	Q ($kg\,s^{-1}$)	F_*
05 Apr	14	1120	3	1.6	B	1335	4	185	0.36	−24	1.9	835	1824	17.9	0.11
01 Jan	10	840	3	1.7	D	676	4	−3	0.23	417	0.0	988	2013	12.8	0.00
04 May	13	800	3	2.6	A	1676	4	244	0.37	−20	2.2	700	1064	10.5	0.03
10 Aug	14	750	8	2.7	B	1659	4	186	0.58	−94	2.0	766	978	18.2	0.04
16 Nov	14	660	10	1.4	C	1288	4	83	0.45	−98	1.4	1142	2174	15.0	0.33
24 Jan	12	640	7	0.8	C	1861	3/6	126	0.56	−129	1.9	962	2581	12.9	0.18
17 Sep	14	580	9	2.7	B	1557	4	162	0.36	−26	1.9	907	1058	20.1	0.06
13 Jul	12	580	9	2.2	B	824	6	239	0.48	−41	1.7	784	1146	15.5	0.15
01 Nov	16	560	10	0.9	D	1303	4	−21	0.35	185	0.0	1147	2845	15.6	0.00
07 Jun	12	560	12	4.8	B	1633	4	247	0.43	−29	2.2	638	600	11.1	0.02
23 Feb	11	560	11	2.2	A	874	4	188	0.25	−8	1.7	765	1365	16.1	0.14
01 Jan	11	560	11	3.0	D	676	4	9	0.19	−72	0.6	988	1116	12.8	1.36
15 Dec	13	550	5	3.3	B	718	4	97	0.24	−13	1.3	807	878	7.9	0.20
17 Sep	13	550	7	3.1	B	1372	4	194	0.31	−14	1.9	919	943	20.1	0.06
13 Jul	15	520	9	2.8	B	1051	6	164	0.41	−39	1.7	780	989	15.5	0.09
28 Mar	9	520	6	6.0	C	589	4	156	0.36	−27	1.4	637	533	8.6	0.09
22 Mar	15	520	11	2.7	C	1957	4	129	0.46	−69	1.9	925	1068	19.5	0.05
22 Mar	9	520	8	5.4	C	754	4	150	0.62	−148	1.5	973	652	19.5	0.11
17 Mar	11	520	7	2.6	C	1277	4	228	0.58	−79	2.0	1008	1110	18.7	0.07
06 Mar	13	520	9	2.0	B	1110	4	200	0.47	−48	1.8	1010	1565	20.6	0.14
08 Jan	12	520	7	5.4	D	742	4	162	0.73	−227	1.5	1114	493	12.3	0.12
01 Nov	15	510	10	1.9	C	1303	4	48	0.49	−223	1.2	1143	2172	15.6	0.08
02 Sep	14	490	10	2.5	D	368	4	31	0.48	−332	0.7	935	1247	20.8	2.07
13 Apr	13	480	8	3.1	B	1257	4	215	0.26	−7	2.0	672	797	6.7	0.04
05 Apr	11	480	8	3.1	B	862	4	234	0.48	−42	1.8	865	1034	17.9	0.10
16 Mar	14	480	7	10.8	D	2275	3/4	173	1.02	−547	2.2	941	427	18.1	0.01
27 Jan	11	480	9	4.6	D	1005	4	149	0.62	−148	1.6	968	751	11.8	0.08
24 Jan	13	480	7	1.7	C	1890	6	116	0.51	−102	1.8	953	1971	12.9	0.09
22 Jan	12	480	7	4.5	D	1075	4	142	0.62	−156	1.6	1195	823	14.9	0.10
16 Nov	15	470	10	1.2	D	1116	4	30	0.60	−656	1.0	1142	2841	15.0	0.88

Notes on Table 3:

(1) Symbols are defined in the text.

(2) Values for F_b, $\bar{h}_c$, and F_* are weighted averages based on the emission rates from each of the three stacks.

(3) Values for the emission rate, Q, represent the total of the three stacks.

Table 4. Frequency distribution and statistical comparison for various variables

Variable	Range	Number of lower 8754 h	Number of top 30 h	Normalized chi-squared statistic
Emission rate ($kg s^{-1}$)	0–5	120	0	
	5–10	1655	3	
	10–15	4021	11	4.7
	15–20	2244	12	(n.s)‡
	>20	716	4	
Receptor distance* (km)	<4	11,863	4	
	4–7	29,178	11	3.5
	7–10	29,509	14	(n.s.)
	>10	12,016	1	
Wind speed ($m s^{-1}$)	<4	1605	23	
	4–6	1878	6	
	6–8	1910	0	65.7
	8–10	1595	0	(<0.01)§
	>10	1547	1	
Synoptic class	1	1560	0	
	2	480	0	
	3	779	1	19.8
	4	4906.5	25.5	(<0.01)
	5	780	0	
	6	248.5	3.5	
Stability class†	A	122	2	
	B	612	11	22.8
	C	1053	8	(<0.01)
	D	3712	9	
Mixing heights (m)†	<500	870	1	
	500–1000	1676	9	
	1000–1500	1550	12	5.6
	1500–2000	964	7	(n.s)
	>2000	439	1	
w_*† ($m s^{-1}$)	<0.5	65	0	
	0.5–1.0	668	2	
	1.0–1.5	929	5	9.6
	1.5–2.0	1085	15	(n.s.)
	>2.0	384	6	
F_*†	<0.09	1408	11	
	0.09–1.0	1311	15	1.5
	>1.0	412	2	(n.s.)
u/w_*†	<1.5	588	13	
	1.5–6.0	2162	14	13.9
	>6.0	386	1	(<0.01)
Similarity category†				
	Near neutral	2160	5	
	Mixed layer	561	6	19.3
	Entrainment	496	6	(<0.01)
	$h_e/h > 1.2$	746	13	

Notes for Table 4:

*Number of hours exceed 8754 because valid concentration data from all receptors were included.

†Only the unstable/neutral hours were included.

‡n.s. means not significant.

§Number in parentheses indicates level of significance.

winds ($<4 m s^{-1}$). For one of the top 30 h, the high concentration was associated with high winds. The distributions of the two data bases were significantly different as determined with a chi-square test.

4.5. *Wind direction*

The analysis of wind direction was approached differently than the other variables. Fig. 4 presents pollution roses which show the direction from which the plume was blowing towards a receptor. To illustrate the prevailing winds in the area, the annual wind rose for 1976 given as an inset in Fig. 4 shows that the winds most frequently blew from the southwest. Another frequent wind direction was from the north, but winds were fairly well distributed in all directions.

The pollution roses attempt to show whether there

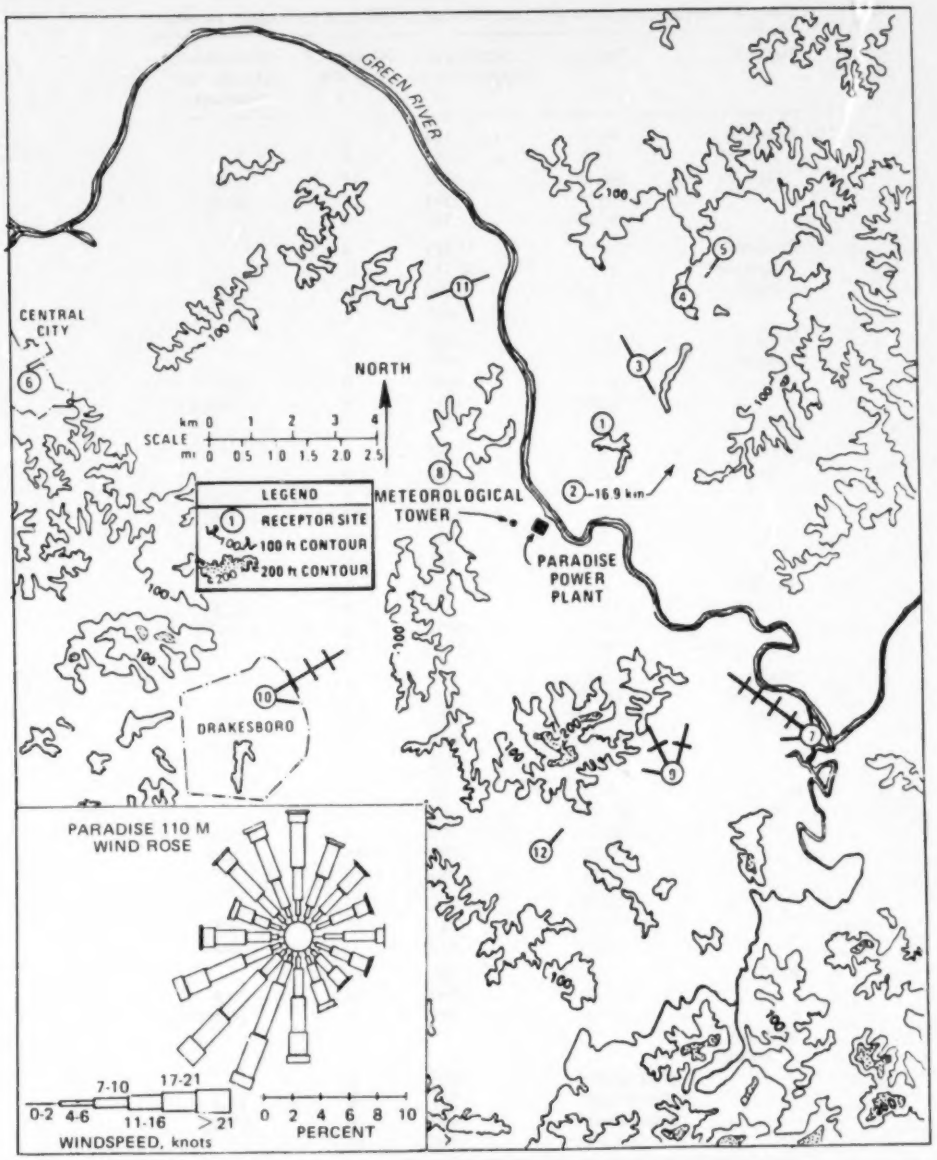

Fig. 4. Pollution roses for the top 30 h data set. The pollution roses are divided into 45 degree sectors and each tick mark represents 1 h. Inset shows the annual wind rose for 1976.

was a preferred wind direction for high concentrations and help demonstrate how accurately on-site wind direction measurements could be used in depicting plume trajectories. Despite the scarcity of receptor locations, it appears that high concentrations can occur with a range of wind directions as illustrated by the number of receptors reporting high concentrations. Only 18 out of 30 h were associated with on-site wind directions that were in a 45 degree sector directed from the power plant to the receptor reporting one of the top 30 h concentrations. All 3-h at receptor 3 were associated with wind directions >45 degrees away from the plant orientation. These 3-h were associated with light wind conditions, when it is difficult to resolve accurately wind direction. It should also be noted that in 1976, no other major sources of SO_2 were known to exist in the area.

4.6. *Stability class*

From the analysis, it was quickly determined that most high concentrations occurred during the daytime with unstable or nearly-neutral atmospheric stability.

Therefore, in comparing the frequency distributions of stability class, only stability classes A–D were included in Table 4. For the lower 8754 h data set, neutral conditions (class D) predominate. However, 33 per cent of the high concentrations were associated with B stability. This difference was confirmed with the chi-square statistic which showed that the two distributions significantly differed at the 1 per cent level of significance.

4.7. *Mixing height*

Comparison of mixing heights for the two data sets revealed little difference. As with stability class, only the unstable/neutral hours were considered in the analysis. Table 4 indicates that the median mixing height is in the range 1000–1500 m for both data sets. The chi-square analysis did not reveal any significant differences between the two distributions.

4.8. *Convective scaling velocity* (w_*)

Values of w_* were divided into bins of 0.5 m s^{-1} from 0.5 to 2.0 m s^{-1}. The median for the top 30 h data set occurred in the range 1.5–2.0 m s^{-1}, while for the lower 8754 h data set, it occurred in the range 1.0–1.5 m s^{-1}. However, frequency distributions for the two data sets were not significantly different.

4.9. *Plume buoyancy* (F_*)

Values of F_* were divided into three categories: non-bumping (<0.09), bumping (0.09–1.0), and likely-penetration (>1.0). These categories are based on the description of F_* by Briggs (1985) who incorporated F_* into a formula for estimating diffusion of a buoyant plume in the convective boundary layer.

Hanna and Paine (1987) suggest the following interpretation of F_*. It is first assumed that the top of the buoyant plume is at 1.5 Δh, where Δh is the plume rise. Briggs' (1984) Equation 8.101 can then be used to redefine Equation (2) as follows:

$$F_* = \left[\frac{1.5\,\Delta h}{h}\right]^{5/3}\left[\frac{2}{9}\right]^{5/3}$$

$$= 0.08\left[\frac{\text{plume rise}}{\text{mixed-layer depth}}\right]^{5/3} \qquad (3)$$

where Δh in Briggs' Equation 8.101 is defined as follows:

$$\Delta h = 3\left[\frac{F_b}{u}\right]^{3/5} H_*^{-2/5}. \qquad (4)$$

Hence a value for F_* of 0.09 indicates approximately when the rise of the buoyant plume begins to be affected significantly by the elevated inversion.

In Table 4, only the daytime hours were included. Bumping and pentration were estimated to occur over 50 per cent of the time for both data sets. The chi-square analysis noted no significant differences between distributions of the two data sets.

4.10. *Ratio of wind speed to convective scaling velocity* (u/w_*)

Deardorff (1970) noted that u/w_* could be related to the turbulent character of the convective boundary layer. Weil and Brower (1984) used u/w_* as an indicator for atmospheric stability in a Gaussian plume dispersion model. In this study, values of u/w_* were divided into three categories: extremely unstable (<1.5), convective (1.5–6.0), and not convective (>6.0). Most of the lower 8754 h data set fell into the convective category. However, the top 30 h data set was about evenly split between the extremely unstable and the convective categories. Because of this trend towards extremely unstable conditions for the top 30 h data set, the chi-square analysis revealed significant differences between the two distributions at the 1% level of significance.

4.11. *Similarity categories*

A novel approach for characterizing diffusion categories was discussed by Gryning *et al.* (1987). They conveniently grouped similarity regimes according to values of h/L and z/h as illustrated in Fig. 5. For this analysis, z was replaced by h_e, the mean effective plume height. Frequencies associated with each similarity regime were determined for the lower 8754 h data set and the top 30 h data set and are listed in Table 4.

As with previous variables, high concentrations were not observed during night-time neutral/stable conditions. Two of the top 30 h did occur during nearly-neutral, very small negative heat flux conditions. Thus, in comparing the top 30 h and the lower 8754 h data set, only the neutral/unstable conditions were considered. It should be noted that surface-based regimes were never associated with any of the data, because the plume was well above the surface layer.

The distributions for the two data sets were not significantly different. However, a large percentage of the unstable/neutral hours were estimated to be associated with h_e/h ratios >1.2. In fact, plume rise for more than 50 per cent of the top 30 h was estimated to be above the mixed layer. This raises a serious concern, because most routine models currently assume zero ground-level impact if the plume is predicted to be above the mixed layer. Therefore, the procedures for estimating plume rise and mixing height were investigated in more detail.

The top 30 h were reanalyzed using more sophisticated plume rise and mixing height procedures. The twice-daily upper-air soundings from BNA were obtained for days containing the top 30 h. The soundings were scrutinized carefully using surface temperatures to determine the depth of the adiabatically-mixed layer. The height at which the potential temperature increased significantly (usually above $+0.0065$ K m^{-1}) was assumed to be the mixing height. Only a few of the mixing heights for the 30 h were altered in this manner. The reanalysis of mixing height allowed temperatures and winds to be gathered

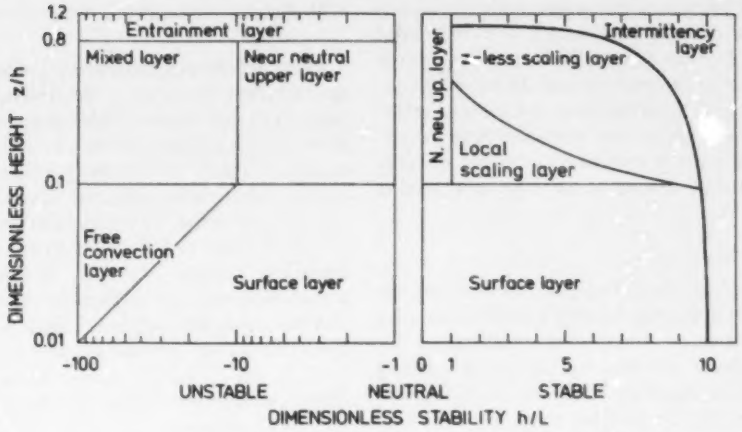

Fig. 5. Similarity classification scheme (from Gryning *et al.*, 1987).

Table 5. Comparison of original and revised estimates of mixing height (h) and effective plume rise (h_e).

Date	Hour	Original h (m)	Revised h (m)	Original h_e (m)	Revised h_e (m)
05 Apr	14	1335	1335	1824	1184
01 Jan	10	676	625	2013	625*
04 May	13	1676	1676	1064	833
10 Aug	14	1659	1550	978	952
16 Nov	14	1288	850	2174	850*
24 Jan	12	1861	1500	2581	1500*
17 Sep	14	1557	1557	1058	1074
13 Jul	12	824	1000	1146	904
01 Nov	16	1303	1050	2845	1050*
07 Jun	12	1633	1633	600	607
23 Feb	11	874	874	1365	874*
01 Jan	11	676	625	1116	625*
15 Dec	13	718	718	878	718*
17 Sep	13	1372	1372	943	957
13 Jul	15	1051	1051	989	931
28 Mar	9	589	589	533	589*
22 Mar	15	1957	1650	1068	1171
22 Mar	9	754	754	652	754*
17 Mar	11	1277	1500	1110	1031
06 Mar	13	1110	1050	1565	1050*
08 Jan	12	742	742	493	742*
01 Nov	15	1303	1303	2172	1303*
02 Sep	14	368	900	1247	900*
13 Apr	13	1257	1150	797	788
05 Apr	11	862	862	1034	794
16 Mar	14	2275	2275	427	398
27 Jan	11	1005	850	751	800
24 Jan	13	1890	1500	1971	1398
22 Jan	12	1075	1200	823	1015
16 Nov	15	1116	850	2841	850*

* h_e was set equal to h because bumping was indicated $0.08 < F_e < 1.0$, and penetration was not predicted.

on a layer-by-layer basis. This information was used in plume rise equations of Briggs (1984) which consider variations of stability with height and partial plume penetration. The original and revised estimates of mixing height and effective plume rise are listed in Table 5.

Using the adjusted values for h/L and h_e/h, the frequency distribution for the top 30 h was determined and is listed in Table 6 along with the original top 30 h frequency distribution. In the revised data set, 21 of the 30 h were associated with h_e/h values greater than 0.80 and therefore were assigned to the entrainment layer

Table 6. Comparison of the original and revised top 30 h data sets with respect to similarity categories

Category	Number or hours in original top 30 h	Number of hours in revised top 30 h	Normalized chi-square statistic
Near neutral	5	1	
Mixed layer	6	8	34.3
Entrainment	6	21 (10,11)*	(<0.01)
$h_c/h > 1.2$	13	0	

* 10 cases having $-h/L \geq 10$ and 11 cases having $-h/L \leq 10$.

category. Unlike the original data set, none of the plume rise estimates for the top 30 h were found to have penetrated into the stable capping inversion above the mixed-layer. As indicated in Table 6, the two distributions are significantly different at the 1% level of significance.

Of the 30 cases having the highest observed concentrations, 18 or about two-thirds satisfied the mixed-layer criteria of $-h/L \geq 10$. Of these 18 cases, 10 were within the entrainment regime. The median mixing depth for the eight cases within the mixed-layer regime was 1553 m. For the 12 cases having $-h/L \leq 10$, only one case was within the near-neutral regime; the other 11 cases were within the entrainment regime. For all 21 cases within the entrainment regime, the median mixing depth was 874 m which is only about half of the value found for the eight mixed-layer cases.

To extrapolate these results to other years is uncertain, as only one year of data was available for analysis. However, based on this limited analysis, we would anticipate high concentrations to be associated with below average mixed-layer depths. On those occasions having more typical mixed-layer depths, highest concentrations would likely be associated with convective conditions when $-h/L \geq 10$.

5. SUMMARY

This paper has attempted to show the usefulness of an air pollution climatology with convective scaling parameters. The analysis has been focused towards offering recommendations on the modeling of tall stacks. While the results of this paper apply to one specific site, the techniques introduced and the general recommendations regarding atmospheric pollution models may be helpful in other situations.

In general, the meteorological conditions producing high concentrations at the Paradise power plant can be described as daytime, neutral/unstable atmospheric stability and usually light winds. The top 30 hourly concentrations usually occurred during the presence of a high pressure system which is typified by a subsidence inversion and light wind speeds. The analysis showed that convective scaling parameters offered some skill in noting the occurrence of high concentrations, but other factors such as the Pasquill stability class showed just as much skill. The analysis also showed some worrisome results regarding wind direction and plant load and offered some helpful results regarding the use of F_* and similarity categories.

Wind direction is a troublesome variable when trying to validate or evaluate atmospheric pollution models for point sources. An error as small as 5 degrees in plume trajectory can alter concentrations by 50 per cent. However, only about 50 per cent of the on-site wind direction measurements indicated a plume trajectory within 45 degrees of the receptor reporting one of the high 30 1-h concentrations. With errors such as this, it is not too surprising that point source models correlate poorly with measurements. Errors in plume trajectories likely occur for several reasons: horizontal variation of the wind, vertical variation of the wind and temporal changes of the wind. Unfortunately, without elaborate measurement systems for resolving the four-dimensional structure of the wind, it will be difficult to minimize errors in wind direction estimates for use in atmospheric pollution models. Therefore, model users and evaluators should be aware of the sensitivity of point source models to small errors in wind direction.

Another area of concern is plant load. The analysis shows that high concentrations can occur during less than full load conditions, thus confirming the modeling results of Irwin and Cope (1979). However, current modeling practice considers emission rates and stack operating parameters associated with full load conditions, because they are thought to be associated with 'worst-case' conditions. Instead, it is recommended that pollution impact for a source such as a power plant be analyzed for a range of load possibilities.

The air pollution climatology revealed major shortcomings in the simplistic treatment of buoyant plume rise as practiced in current air pollution modeling, such as E.P.A. (1977). Given a stability class and a stack top wind speed, the models compute plume rise irrespective of the depth of the mixing layer or the strength of the capping inversion. This approach resulted in suggesting that plume rise for 15 of the top 30 h was above the mixed-layer depth. This result is unrealistic.

Briggs (1984) has introduced plume rise equations which attempt to deal with the vertical temperature and wind speed structure of the atmosphere. Use of these equations suggested that plume was within the mixed layer for all 30 h of the highest concentrations. For 21 of these the plume was predicted to be within the entrainment regime. Cases within the entrainment zone would likely involve a phenomenon known as bumping. Diffusion equations that account for bumping were introduced by Briggs (1985). As a simple test of this approach, maximum ground-level concentrations were computed for 15 of the top 30 h using Equation (25) from Briggs (1985):

$$\chi_c = 0.03Q\, w_*^2/(F_b h) \qquad (5)$$

where χ_c is the maximum ground-level concentration and the other terms were defined in section 3. The 15 h were associated with F_* values which ranged from 0.09 to 1.0. The median concentration predicted with Equation (5) was 1348 $\mu m\, m^{-3}$ and compares quite closely with the observed median concentration of 1362 $\mu g\, m^{-3}$.

Towing tank studies by Deardorff and Willis (1984) clearly show the non-Gaussian vertical distribution of the buoyant plume in the convective boundary layer. Using the results of the towing tank studies and a limited amount of field data, Briggs (1985) proposed analytical expressions incorporating the effects of plume buoyancy (including Equation (5) above) in the convective boundary layer which can be used to improve tall stack models. The analytical expressions of Briggs simulate the enhanced lateral spreading that the buoyant plume experiences when it bumps against the elevated inversion. In addition, they account for the tendency of the plume to remain well intact just below the inversion and to be slowly dispersed down towards the surface by convective eddies. The net effect is reduced peak ground-level concentrations compared to passive plume dispersion formulations, but the elevated concentrations predicted with the bumping formulation tend to persist for several kilometers. This helps to explain the wide range of distances associated with high concentrations at Paradise and other power plants (Bowne and Londergan, 1983).

Analysis of data from the Paradise power plant has shown the importance of knowing plume behavior in a convective boundary layer. It appears that the elevated short-term SO_2 concentrations at Paradise were closely linked to the interaction of the plume with the daytime elevated inversion. It remains to be determined whether this finding can be generalized to other sources and climatic regimes. In the meantime, it is recommended that additional improvements and evaluation studies be made with atmospheric pollution models to consider buoyant plumes in the unstable boundary layer.

Acknowledgements—The author would like to acknowledge Dr Sven-Erik Gryning who gave permission to use Fig. 5 and Ms Diane Rumsey who assisted in the data analysis. The author especially wishes to thank Mr. John Irwin for his encouragement and review of this study.

Disclaimer—Although the research in this article has been funded by the United States Environmental Protection Agency, it has not been subjected to agency review and therefore does not necessarily reflect the views of the agency and no official endorsement should be inferred.

REFERENCES

Bowne N. E. and Londergan R. J. (1983) Overview, results, and conclusions for the EPRI plume model and development project: Plains site. Electric Power Research Institute, Palo Alto, California, EPRI EA-3074.

Briggs G. A. (1975) Plume rise predictions. In *Lectures on Air Pollution and Environmental Impact Analysis*, (edited by D. A. Haugen) Amer. Meteorol. Soc., Chapter 3, pp. 59–111. Boston, MA.

Briggs G. A. (1984) Plume rise and buoyancy effects. In *Atmospheric Science and Power Production* (edited by D. Randerson) U.S. Dept of Energy DOE/TIC-27601. [Available from NTIS as DE84005177.]

Briggs G. A. (1985) Analytical parameterizations of diffusion: the convective boundary layer. *J. Clim. appl. Meteor.* **24,** 1167–1186.

Deardorff J. W. (1970) Preliminary results from numerical integrations of the unstable planetary boundary layer. *J. atmos. Sci.* **24,** 1209–1211.

Deardorff J. W. and Willis G. E. (1984) Ground-level concentration fluctuations from a buoyant and a non-buoyant source within a laboratory convectively mixed layer. *Atmospheric Environment* **14,** 1451–1458.

Grying S. E., Holtslag A. A. M., Irwin J. S. and Sivertsen B. (1987) Applied dispersion modeling based on meteorological scaling parameters. *Atmospheric Environment* **21,** 79–89.

Hanna S. R. and Paine R. J. (1987) Convective scaling applied to diffusion of buoyant plumes from tall stacks. *Atmospheric Environment* **21,** 2153–2162.

Hanna S. R., Weil J. C. and Paine R. J. (1987) Testing of a new plume dispersion model with the Kincaid and Bull Run data. Presented as paper 87-73.4 at Air Pollution Control Association Annual Meeting, New York, 21–26 June.

Holtslag A. A. M. and van Ulden A. P. (1983) A simple scheme for daytime estimates of the surface fluxes from routine weather data. *J. Clim. appl. Met.* **22,** 517–529.

Holzworth G. C. (1987) Air pollution climatology. In *The Encyclopedia of Climatology* (edited by J. E. Oliver and R. W. Fairbridge). pp. 27–38. van Nostrand Reinhold Company, New York.

Irwin J. S. and Cope A. (1979) Technical note: maximum surface concentrations of sulfur dioxide from a moderate-size steam-electric power plant as a function of power plant load. *Atmospheric Environment* **13,** 195–197.

Lee C. B. (1986) Simple model and climatological aspects of the structure of the convective boundary layer. *Atmospheric Environment* **20,** 705–714.

Ning D. T. and Yap D. (1986) Climatology of convective boundary-layer parameters over Ontario, Canada. *Atmospheric Environment* **20,** 2315–2323.

Paumier J., Stinson D., Kelly T., Bollinger C. and Irwin J. S. (1986) MPDA-1: a meteorological processor for diffusion analysis. EPA/600/8-86/011, U.S. Environmental Protection Agency, Research Triangle Park, NC. [Available from NTIS as PB86-171-402/AS.]

Pierce T. E. (1986) Estimating surface concentrations from an elevated buoyant plume in the limited-mixed convective

boundary layer. Conference volume, *Fifth Joint Conf. on Applications of Air Pollution Meteorology*, Chapel Hill, Amer. Met. Soc., 331–334.

Turner D. B. (1964) A diffusion model for an urban area. *J. appl. Met* **3**, 83–91.

U. S. Environmental Protection Agency (1977) User's Manual for Single-Source (CRSTER) Model. EPA-450/2-77-013, Research Triangle Park, NC.

Venkatram A. (1980) Dispersion from an elevated source in a convective boundary layer. *Atmospheric Environment* **14**, 1–10.

Weil J. C., Corio L. A. and Brower R. P. (1986) Dispersion of buoyant plumes in the convective boundary layer. Conference volume, *Fifth Joint Conf. on Applications of Air Pollution Meteorology*, Chapel Hill, Amer. Met. Soc., 335–338.

Weil J. C. and Brower R. P. (1984) The Maryland PPSP dispersion model for tall stacks. *J. Air Pollut. Control Ass.* **34**, 818–827.

Yu C. H. and Pielke R. A. (1986) Mesoscale air quality under stagnant synoptic cold season conditions in the Lake Powell area. *Atmospheric Environment* **20**, 1751–1762.

NOTICE

This document has been reviewed in accordance with U.S. Environmental Protection Agency policy and approved for publication. Mention of trade names or commercial products does not constitute endorsement or recommendation for use.

This article documents research that was conducted under the auspices of the U.S. Environmental Protection Agency (USEPA). As an arm of the government, the USEPA has a paid up, non-exclusive, irrevocable, worldwide license to reproduce, prepare derivative works, and distribute to the public all of the material contained herein, and to grant others acting on its behalf the right to do so. The USEPA grants to the National Technical Information Service, Department of Commerce, the right to act as its agent in the distribution of this material.